Mohiuddin, Zeeshan; Stokes, Yvonne Marie; Haghighi, Manouchehr
Pore level simulation of miscible injection with gravity domination
Energy Procedia, 2013; 37:6885-6900

Available online at www.sciencedirect.com

SciVerse ScienceDirect

Energy Procedia 37 (2013) 6885 – 6900

Energy Procedia

GHGT-11

Pore level simulation of miscible injection with gravity domination

Zeeshan Mohiuddin[a]*, Yvonne Stokes[b] and Manouchehr Haghighi[a]

[a] *Australian School of Petroleum, The University of Adelaide,Adelaide, Australia*
[b] *School of Mathematical Sciences. The University of Adelaide , Adelaide, Australia*

Abstract

Gravity assisted miscible CO_2 injection into oil reservoirs is an efficient method of enhancing oil recovery. CO_2 injection into aquifers for sequestration purposes is another application of miscible displacement under gravity control. This paper reports pore scale simulation studies to determine the role of different parameters on the frontal stability of the miscible displacement process under gravity.

The simulation studies were performed using the Finite Element Analysis technique. The simulation model was initially validated by matching results with flow visualization experimental studies using glass micromodels. The Navier-Stokes, continuity and convection-diffusion equations were used in the simulation instead of ideal Darcy law. Wide ranges of parameters applicable for Enhanced Oil Recovery and CO_2 sequestration have been used in the sensitivity study. Dip angles(θ) between 0^o and 180^o (for up-dip and down-dip situations), different domain velocities, density differences of 50 to 900 kg/m^3 between the injecting and displaced fluids and viscosity ratios from 1 to 50 (to include light and heavy oils) have been investigated. Snapshots were captured in each simulation case for visual comparison of the frontal advancement. In addition, breakthrough saturation was plotted against cos (θ) to quantify the competition between viscous and gravity forces in gravity dominated miscible displacement process.

The pore scale study suggests that stability of a miscible process can be influenced by several factors. When gravity acts in favor of displacement and there is a moderate to large density difference, angular tilt is the most important parameter influencing displacement. When the density difference is small then the mobility ratio and flow velocity also play a role. When gravity opposes displacement and buoyancy forces are dominating, results show little sensitivity to the actual tilt angle. Better displacement is seen for lower density difference and for higher flow velocity, while, again, the mobility ratio only impacts on displacement when the density difference is quite small.

Selection and/or peer-review under responsibility of GHGT

* Corresponding author. Tel.: +61406146513, +61883034298; fax:+61883034345.
E-mail address: zmohiuddin@asp.adelaide.edu.au, zeeextra@yahoo.com.

1876-6102
Selection and/or peer-review under responsibility of GHGT
doi:10.1016/j.egypro.2013.06.621

1. Introduction

Miscible gas injection is an effective method of enhanced oil recovery (EOR). Efficiency of the miscible gas injection process relies on the contact of injected gas with the trapped oil. It is because of the fact that if the injected gas does not made contact with the inplace fluid, the displacement of un-contacted oil cannot occur. However less viscosity and density of injected gas restricts this contact with oil even in homogeneous reservoirs and causes instabilities at the gas oil interface [1]. The inherited problems of miscible flooding could be reduced by injecting a less dense fluid in the direction parallel to gravity i.e. $\theta=0^o$ and not in the perpendicular direction i.e. $\theta=90^o$and thus couples the conventional miscible EOR with a gravity drainage process. When a less dense fluid is injected into a dense fluid at $\theta=0^o$, the gravity forces segregates the injected gas to stay at the top of oil column due to density difference and pushes the oil underneath it. The gravity forces dominates the viscous forces which favors the stability of the displacement process [2].Therefore, miscible gas assisted gravity drainage (MGAGD) helps to minimize gravity tongues and stabilizes the viscous fingering to increase the sweep efficiency[3]. Besides, this EOR process offers additional application of CO_2 sequestration in subsurface formation [4]. To date MGAGD process has been studied [4, 5] and used successfully in various fields [6-9] across the world.

Although this approach promises significant benefits over other conventional miscible displacement processes, one must realize that its efficiency may be sensitive to various parameters. Moreover any process has some limitations and instability will arise when the process is not implemented correctly. Instabilities start at pore level and so that pore scale knowledge is important to estimate the efficiency of this process which, in return, helps to develop better understanding at large scale. Pore level information can be utilized to determine the areal and vertical sweep efficiencies. In the domain of MGAGD, several experimental studies [2, 3, 10-19] have been reported in past. However experimental studies have some limitations and operational challenges, such as lengthy experimental time, which limits the execution of experiments. Furthermore, experimental studies contains risks which are associated with unavoidable human, instrumental and post processing etc. which affects the precision and accuracy of the results. Therefore, pore scale simulation approach can be used to obtain the required results. Simulation allows more flexibility for testing various scenarios to evaluate various different schemes. However reliability of simulation results relies on validation of the simulation model. Thus a simulation model must be validated by comparing simulation and experimental results, before used for any prediction.

The relevance of pore level fluid flow simulation has been appreciated since Fatt [20] compared the capillary pressure, relative permeability and electrical resistivity of actual rock and a capillary tube network to establish concurrency between this capillary network and the real porous media. Since then, numerous studies have been reported [21-27]. A network model approach is often used which is a network of small pore bodies, interconnected with throats or capillaries to represent void spaces of a porous rock. The pores and throats are spatially arranged based on some defined arrangement such as rectangular, diamond, hexagonal etc. The pore and throat shapes are selected to model specific problem. Pore and throat size are generated randomly[24] or based on some experimental evidence[28]. Desired physics was then assigned to calculate quantities such as pressure through material balancing at each node. Results obtained from this simulation are matched with available experimental data and the geometric features of the network model are tuned to improve the comparison with experiments. Figure 1 shows the schematic of a pore network where a central pore is attached to 4 other pores through throats.

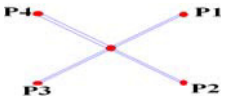

Figure 1. Schematic of a pore network model

It is however obvious that this kind of modeling offers uncertainties because the real porous network is over simplified by a stick and ball model in which the sticks and balls sizes and position are randomly generated values. Thus the actual porous mechanism cannot be truly captured by the use of network model. Besides, since the actual geometry is unknown, several different configurations can produce similar result [22] which make this process more dubious. Furthermore, to determine the actual porous arrangement, only few parameters are matched therefore there are some chances that other parameters might not matched compared to the parameter under observation. Nevertheless all the experimental studies are accompanied with some sources of operational/unavoidable errors and therefore relying on only experimental matching cannot provide a decent network model which represents the actual porous geometry. In addition, since a throat is considered as a small capillary or a small diameter tube, pipe flow equations (Hagen–Poiseuille approximation) were assigned to solve the flow mechanisms. Thus, solving a pipe flow for a porous geometry is not a good idea. Few attempts have been made [24, 29] to simulate MGAGD at pore scale however, these studies were also based on pore network pipe flow modeling. Thus the network model was tuned to acquire the experimental results. Furthermore the experimental studies were conducted using a method, such as glass beads, which cannot be replicated. Besides, sensitivity studies were based on only perfectly upward or downward injection and no tilt angle was considered. In fact, the angular tilt is one of the most important parameter in MGAGD as no ideal scenario exists in real world. Therefore present research was conducted to fill gaps in past experimental and simulation studies.

2. Experimental study

Glass micromodel experiments were conducted to visualize the flow in the porous media. Two glass micromodels patterns were generated through MATLAB and etched on a glass plate. Details of the fabrication of glass micromodels can be found in[18]. The patterns geometries are shown in Figure 2. Pattern 1 contains 8x10 grains of 0.7cm diameter with mean distance of 0.77cm between any two circles centers with the standard deviation of 0.025cm. Pattern 2 contains 11 x 14 grains of 0.5cm diameter with mean distance of 0.58cm between any two circles centers with the standard deviation of 0.0266cm.

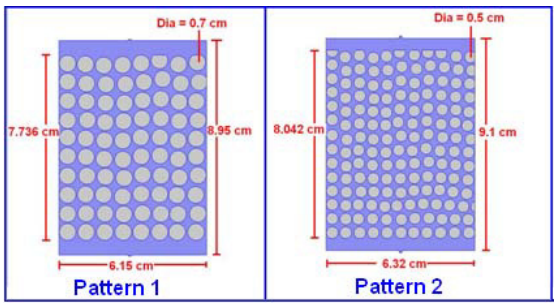

Figure 2. Schematic of patterns used in experimental study

Iso-octane (0.51 cP , 0.69 kg/m^3) and butanol (3cP, 0.81 kg/m^3) were used as injected and inplace fluids respectively as they are soluble in one another at room condition and the mobility(5.88) and density (1.18) ratios of these two fluids are comparable with medium API oil and CO_2 at reservoir conditions[30]. Iso-octane was dyed red so that it can be distinguished with the colorless butanol. The injection of isooctane was carried out at the flow rate of 0.005 cm^3/min in the first and second patterns. The experiments were conducted at an orientation of 0^o, 30^o, 45^o, 60^o and 90^o with respect to the vertical. The images were captured during the experimental studies at particular time intervals. The captured images

were then processed in MATLAB to estimate the concentration in the porous domain. Figure 3 shows the steps involved in the image processing of a captured image(details can be found in[19]).

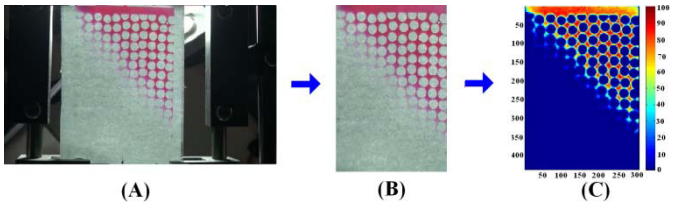

Figure 3. (A) Image captured (B) image cropping (C) image processing

Due to the inherited experimental errors and limitations, explained earlier, a simulation study was conducted so that detail sensitivity studies can be conducted.

3. Numerical simulation

For modeling and flow simulation, COMSOL Multiphysics V4.2a was used. MATLAB generated grain patterns that were used in the experimental study were imported into COMSOL Multiphysics so that direct comparison between experiment and simulation could be made. Thus actual geometry was used in the simulation study which omits any uncertainty about the porous geometry. To simulate the inlet and outlet connections, a small inlet connection was added to the geometry. Meshing across the whole domain was performed in COMSOL. Figure 4 shows the two geometries used in COMSOL simulation.

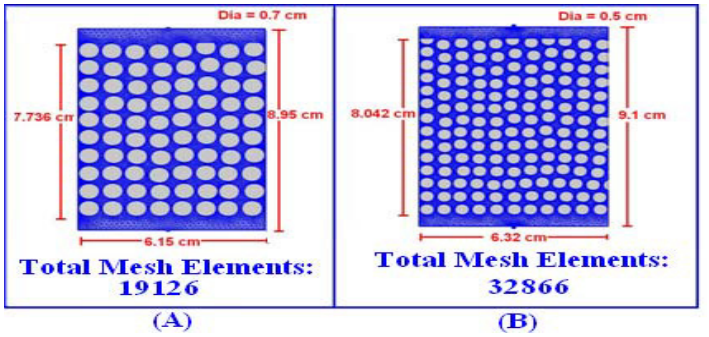

Figure 4. Geometry used in simulation for (A) pattern 1 and (B) pattern 2

3.1. Mathematical model

Flow simulation in COMSOL was performed throughout the flow domain. The injected fluid (solute) and the inplace fluid (solvent) were modeled as a single incompressible phase having a volume fraction C of solute. Continuity and unsteady Navier-Stokes equations were used to calculate the velocity.

$$\nabla . v = 0 \tag{1}$$

$$\rho \frac{\partial v}{\partial t} - \mu \nabla^2 v + \rho (v . \nabla) v + \nabla P - \rho g (\hat{j}) = 0 \tag{2}$$

Where ρ= Density, μ= Viscosity, P= Pressure, g= Gravitational Acceleration and $(\hat{j})$ = (sinθ, cosθ)

The solution of Equations 1 and 2 provides the pore velocities (v) at each node of the finite-element model. The simulations are at the pore scale, in that grain boundaries were explicitly modeled as no-slip boundaries. In addition both of the side walls of the model were modeled as no slip boundary. Both initial velocity and pressure in the porous domain were assumed to be zero. The top inlet connection of 2 mm in length was added to simulate the effect of syringe inlet connection which was used in experiments. Solute, with volume fraction C=1, was continuously injected at a constant velocity from inlet connection. At the injection boundary there are no grains so that the mean pore velocity must increase within the pores as grains are encountered. Pore velocities can vary significantly over small distances depending on the size of the grains and pores. The pressure at the outlet is constant at atmospheric pressure. The density and viscosity of the fluid in the model was modeled as a linear function of concentration i.e.:

$$\rho = C*\rho_{injected} + (1-C)*\rho_{inplace} \quad (3)$$

$$\mu = C*\mu_{injected} + (1-C)*\mu_{inplace} \quad (4)$$

where C is the concentration (or volume fraction) of the injected solute and $\rho_{inplace/injected}$, and $\mu_{inplace/injected}$ are the densities and viscosities of butanol and iso-octane respectively. Once pore velocities are determined, the solute concentration (C) was determined by solving the time-dependent convection-diffusion equation:

$$\frac{\partial C}{\partial t} + \nabla.(-D_o \nabla C) + v.\nabla C = 0 \quad (5)$$

D_o correspond to the diffusion coefficient between butanol and iso-octane (i.e. 6.57×10^{-10} m^2/s). The boundary condition on all the grain boundaries and both the side walls was no diffusive flux. The no slip boundary condition in the fluid flow model ensures that no mass transport occurs through grains boundaries and through the side walls. At the outlet boundary, convection was assumed to be the dominating transport mechanism and diffusive transport was set to zero i.e.

$$D_o \nabla c = 0 \quad (6)$$

The initial concentration of solute (iso-octane) was assigned 0 mol/m^3 i.e. the domain was completely filled with solvent (butanol). However the concentration of solute at the inlet boundary was set to 1 mol/m^3 which represents the injection of iso-octane. The velocity "v" in equation 5 is obtained from the Navier Strokes flow model. The flow and concentration models are solved simultaneously at each time step to yield the velocity and concentration of the fluids over time.

4. Experiment and simulation result matching

The matching parameter in the simulation study was concentration of iso-octane (injected fluid) in the porous domain. This concentration was matched using two different techniques; (a) qualitative and (b) quantitative matching.

4.1. Qualitative matching

Qualitative matching refers to the matching of the front advancement in the porous domain. During the experimental study, images were captured at fixed time steps. Since glass micromodel is transparent, the dyed iso-octane and butanol can be distinguished. Captured images were processed and concentration

profile was assigned as described in[19]. Similarly snapshots were captured from the corresponding simulation case at the same time steps. The experimental processed image was then matched with the simulated image so that a direct comparison of front advancement can be made. This type of comparison provides true matching of the simulation and experimental results in terms of frontal advancement.

4.1.1. Qualitative matching in the first pattern

The experimental and simulation results in the qualitative matching are shown in Figure 5.

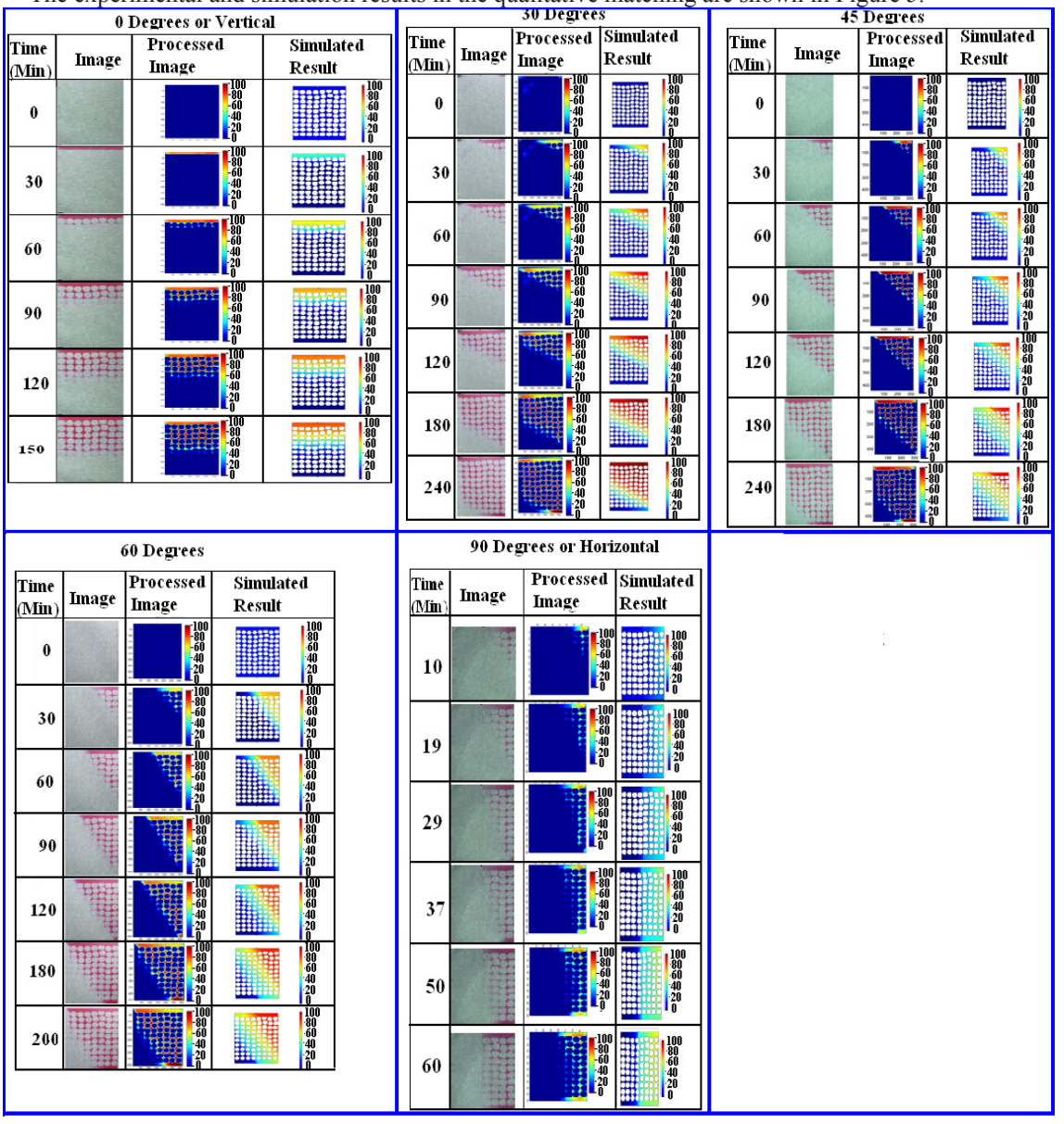

Figure 5. Qualitative experimental and simulation matching for the first pattern

As described in section 2, the iso-octane was injected in the first micromodel at the rate of 0.005 cm^3/min at 0^o, 30^o, 45^o, 60^o and 90^o with respect to the vertical. The experimental and simulation results comparison shown in Figure 5 demonstrates that the trend of front propagation is similar in both experiment and simulation. However, towards the end of the experiments, the front propagates a bit faster which is due to the limitation of the glass syringe used for injection purposes. The inner diameter of the glass syringe become slightly reduces at the upper end of the syringe in order to have a good seal, so that the injection rate becomes disturbed a bit. This is visible in the pictorial matching as towards the end of experiment, the front propagation becomes fast.

4.1.2. Qualitative matching in the second pattern

The experimental and simulation results in the qualitative matching are shown in Figure 6 which shows that the trend of front propagation is similar to that observed for pattern 1. Also, the experiment and simulation show similar behavior. Besides a little separation towards the end of experiment, the overall match was good. The late time mismatch is for the same reason as described in section 4.1.1.

The experiment and simulation results shows that the breakthrough in the vertical case occurred at larger time compared to other cases due to the favorable gravitational force. However when the micromodel was tilted, the breakthrough occurs earlier than in the vertical case. Furthermore the percentage of unswept butanol at the breakthrough increases when the tilt angle is increased.

4.2. Quantitative matching

Quantitative matching refers to the matching of experiment and simulation domain concentration values rather comparing them pictorially. Thus concentration of the injected fluid was obtained in both experiment and simulation at different time steps and then the values were compared.

The concentration of the injected fluid in the experiments was calculated through image processing. In order to get value of concentration, the micromodel was flooded with iso-octane until all the pores are completely filled. An image was captured and processed. This value of solute concentration obtained was considered to have the maximum solute concentration. The other captured images were then compared with the estimated maximum solute concentration to obtain concentration of solute at particular time. It is to be noted that this is an estimated value and might have some operational error(s). Therefore qualitative matching could be preferred over quantitative matching because the trend of front advancement is used to be compared rather than relying on estimated values.

The concentration of the injected fluid in simulation was obtained through the surface integration of concentration of the iso-octane throughout the flow domain. This provides the average concentration of iso-octane at different time intervals.

The quantitative matching of the experimental and simulation results for the first pattern is shown in Figure 7. The simulated and experimental saturation of injected fluid in the domain is plotted against the elapsed time. For all the tilt angles, the trend of both simulation and experiment was found similar specially for the early time. The late time profiles did not matched well due to the same reason as described before that towards the end of the experiments, the front propagates bit fast due to the limitation of the glass syringe used for injection purposes.

The quantitative matching of the experimental and simulation results for the second pattern is shown in Figure 8 which describes that the trend of concentration of iso-octane in experiment and simulation is similar. The exact values are not matched due to over estimation of concentration during the image processing.

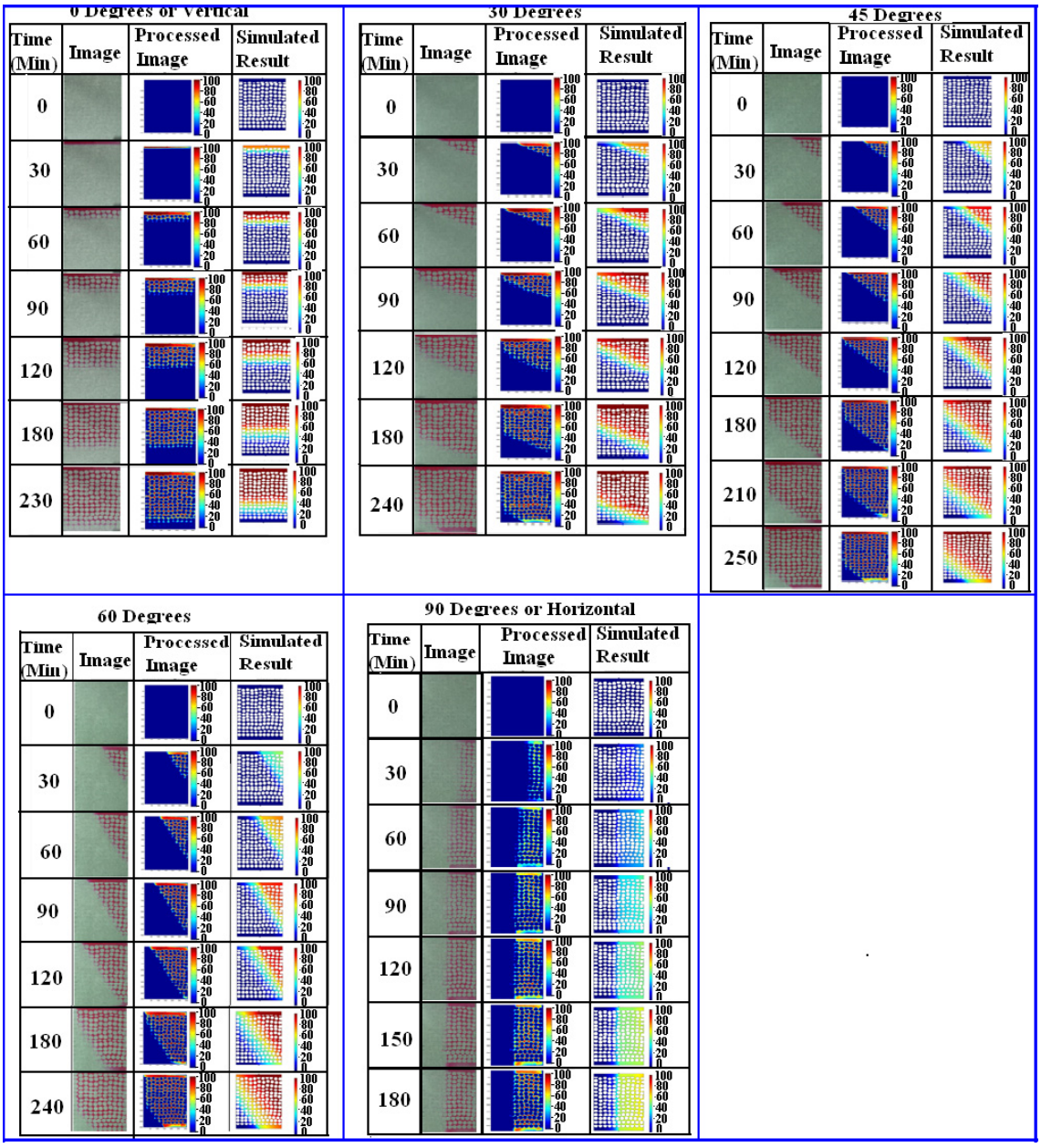

Figure 6. Qualitative experimental and simulation matching for the first pattern

Besides few exceptions due to the image processing errors and/or numerical disturbance, the overall comparison of experiments and simulation through qualitative and quantitative approach shows the similar behavior. This validates the assigned physics and the boundary conditions used. This similar behavior might be due to the fact that exact geometry of porous material has been used in simulation and experimental work. Furthermore, more exact physics has been assigned in the porous media rather relaying on the pipe flow equations. Therefore the applied physics was used in further sensitivity analysis.

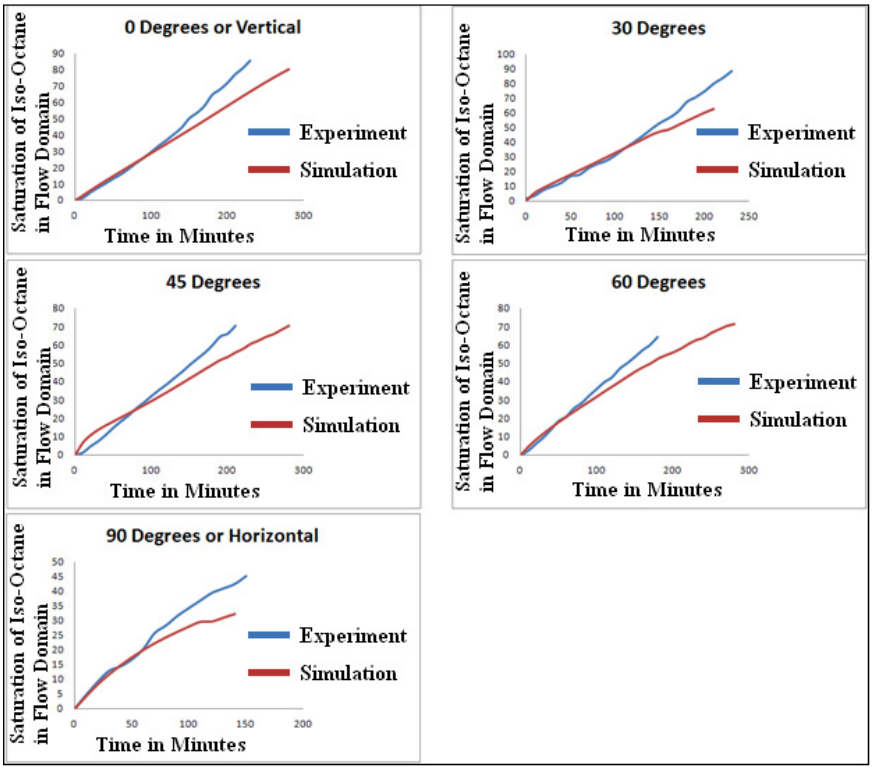

Figure 7. Quantitative experimental and simulation matching for the first pattern

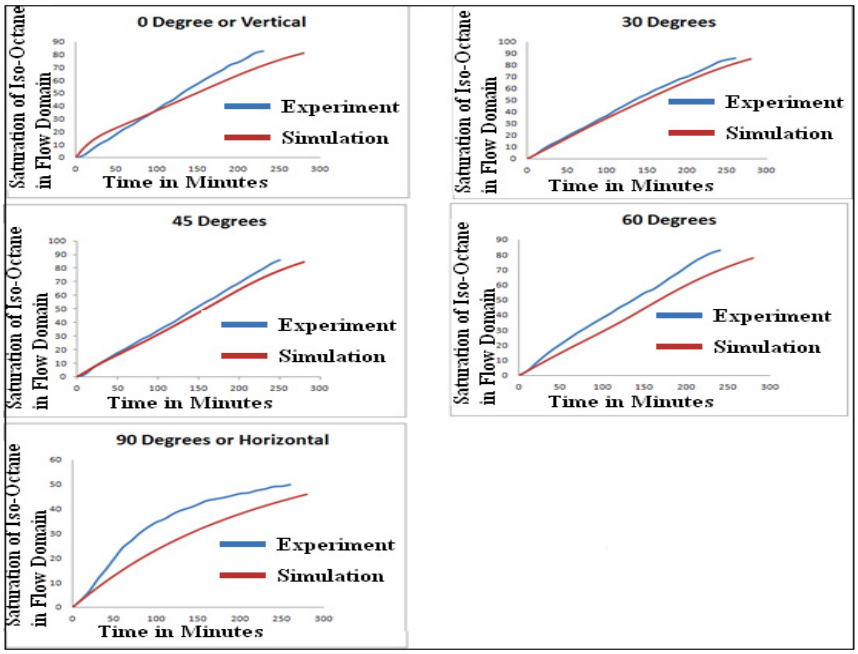

Figure 8. Quantitative experimental and simulation matching for the second pattern

5. Sensitivity Analysis

A sensitivity analysis was performed to determine the effect of different parameters on the stability of gravity dominated miscible displacement. The sensitivity analysis for this study has been divided into two categories:

5.1. Sensitivity Analysis Based on Mobility, Density and Angle of Tilt

The aim of this study was to identify the role of fluid properties (density and viscosity) on the gravity dominated miscible displacement at different angles of tilt at a fixed velocity. Pattern 2 described in section 3 was used in this sensitivity study. An inlet velocity of $7.3\text{x}10^{-5}$ m/s was calculated using equation 10 which corresponds to a domain velocity of 0.8 ft/day. This value for domain velocity was selected because the average velocity in real porous media can vary from 0.1 ft/day to 1.0 ft/day[31], therefore a velocity of 0.8 ft/day was deemed appropriate.

$$Inlet\ Velocity = \frac{\text{Domain Velocity x Effective Width x Depth of Micromodel}}{\text{Inlet Port Cross Sectional Area}} \tag{10}$$

where domain velocity=0.8ft/day or $2.8\text{x}10^{-6}$ m/s, depth of micromodel=4.4 $\text{x}10^{-4}$ m (from experimental study), inlet port cross sectional area= $4.4\text{x}10^{-7}$ m^2 (from experimental study) and

$$Effective\ Width = \frac{Surface\ Area\ of\ the\ Porous\ Domain\ (Calculated\ in\ COMSOL)}{\text{Total Area of the Porous Domain (i.e Actual Width x Actual Actual Height)}} \text{x Actual Width} \tag{11}$$

$$= \frac{2.12\text{x}10^{-3}}{(8.04\text{x}10^{-2})\text{x}(6.33\text{x}10^{-2})}\ \text{x}6.33\text{x}10^{-2} = 2.633\ \text{x}\ 10^{-2}\text{m}$$

Sensitivity studies were performed for nine angles of tilt with respect to the vertical plane (i.e. 0^o, 30^o, 45^o, 60^o, 90^o, 120^o,135^o,150^o and 180^o), four mobility ratios (i.e. 1,3,10 and 100) and seven density differences (50, 100, 200 , 400 , 600, 800 and 900 kg/m^3). Diffusion coefficient of CO_2-oil system ($2\text{x}10^{-9}$ m^2/s) was used. The obtained results were divided into two regions:

5.1.1. Region 1

The region 1 refers to a region where the gravity forces acts in favour of the fluid displacement i.e. $0 \geq \theta \geq 90$. Snapshots given in Figure 9 shows the saturation profiles of the injected fluid at break through. The breakthrough profiles in Figure 9 compare the effect of density change and angular tilts for mobility ratios (M) of 1 and 100 respectively. The breakthrough saturation (S_b) in present study is defined as saturation of injected fluid in the porous domain when 0.2 mol/m^3 concentration of injected fluid is sensed at the outlet grain boundary. The larger value of S_b represents more recovery and better displacement. Figure 9 shows that effects of overriding appeared in all density differences cases when the tilt angle is increased from 0^o with respect to vertical. The lighter injected fluid tends to override the dense insitu fluid, leaving small to large proportions of unswept zones depending on the increase in angular tilt.

By comparing cases of density difference 50 kg/m^3 and 200 kg/m^3 at 0^o with M=1, it can be observed that when the density difference is increased from 50 to 200 kg/m^3, a very little increment in S_b is witnessed and more inplace fluid was displaced. However, when the tilt angle is increased from 0^o to 45^o, the scenario becomes reversed and less fluid was displaced if the density is increased from 50 to 200 kg/m^3. It is because of the fact that when the density difference is high at 0^o, gravity segregation helps the

displacement however at tilt angle of 45°, more overriding occurs as the less dense fluid tends to override. The trend remains same if the tilt angle is progressively increased to 90°.

If a comparison is made between cases of M=1 and M=100 with the density difference of 50 kg/m^3, it can be observed that increase in M from 1 to 100 causes more channelling. However if a comparison is made between cases of M=1 and M=100 with the density difference of 200 and 900kg/m^3, it can be observed that increase in M from 1 to 100 causes little or no effect and the corresponding images shows small difference. Thus, the effects of mobility are more prominent if the density difference is small however, when the density difference is high, the viscosity effects become suppressed and the gravity overriding phenomenon dominates. For example at 90°, when M is increased from 1 to 100, more viscous fingering with gravity override can be seen in cases of 50 kg/m^3 compared with the cases of 200 kg/m^3.

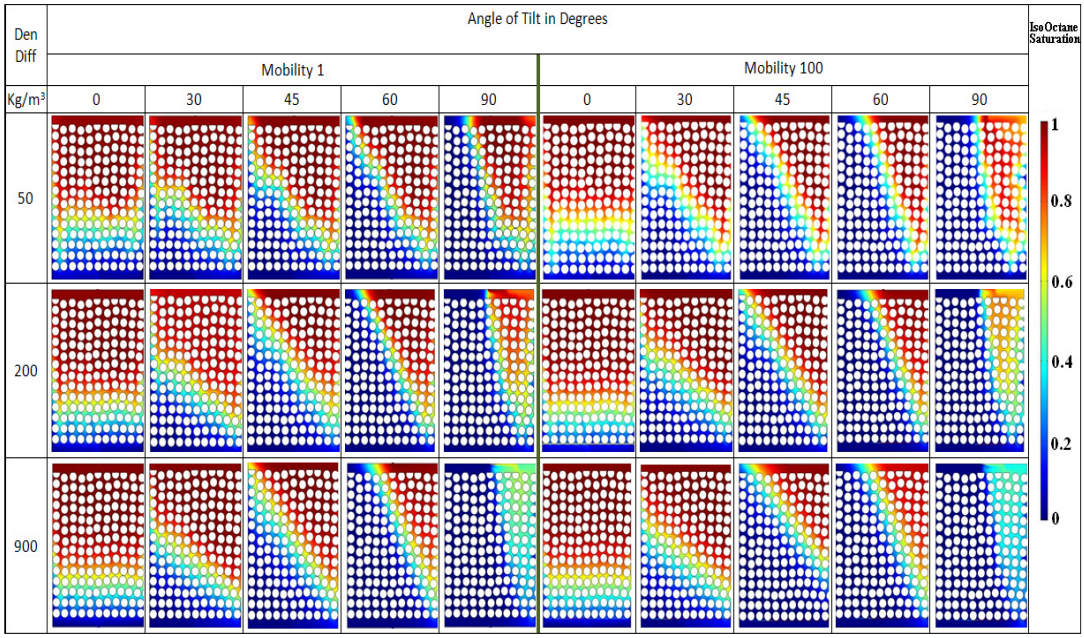

Figure 9. Comparison of different cases of region 1 with mobility ratio 1 and 100

Figure 9 also shows that if the density difference is 200 kg/m^3 or 900 kg/m^3 then little or no effect can be seen among the propagation fronts of respective angular tilts regardless of the M. For example, a little or no change has been observed for 45° cases of 200 kg/m3 and 900kg/m^3 at mobility ratio of 1 and 100. All four images seem similar to each other which supports the concept defined above that when the density difference is high, the gravity effects are more prominent and regardless of viscosity contrast, the propagation of front remains same and gravity override prevails the viscous channeling.

Figure 10 shows the plot of breakthrough saturation (S_b) versus cos (θ), where θ is the angle of tilt in degrees with respect to the vertical plane.

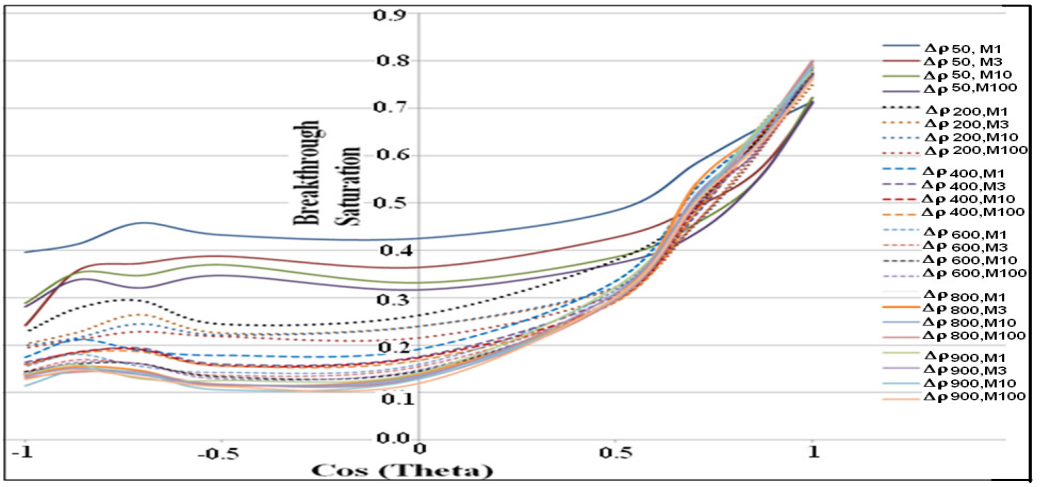

Figure 10. Breakthrough saturation Vs cos (θ) for range of mobility ratios and density differences

Figure 10 further elaborates the concept defined in the above paragraphs that the role of the angle of tilt θ is found to be the most important parameter especially when the density difference is equal or greater than 200 kg/m^3. As the angle of tilt increases from 0° (or cosθ=1), the breakthrough saturation starts to decrease. This trend continues as the angle of tilt approaches 90°(or cosθ=0). All the other density difference curves falls on top of this curve regardless of the change of mobility ratio which signifies the fact that when the density difference is large, density forces are dominating and the effects of gravity are more predominant, which causes the decrease in the breakthrough saturation. When the density difference is less than 200 kg/m^3 the mobility ratio between the in-place and the displacing fluid has an increased effect and the displacing and in-place fluids are behaving similarly because the density difference between the two fluids is less.

5.1.2. Region 2

The region 2 refers to a region where the gravity forces acts against the fluid displacement i.e. 90>θ≥180. Pore scale images outlined in Figure 11 shows saturation profiles of the injected fluid at break through. These breakthrough profiles compare the effects of density change and angular tilt between 120^o and 180^o with viscosity ratios of 1 and 100 respectively. Figure 11 shows that at fixed density difference the angle of tilt (θ), does not have a significant effect as was observed in region 1. It is because of the fact that when a light fluid is injected against the gravity then it tends to rise for a breakthrough. More fluid becomes unswept if the density difference is increased due to more buoyancy forces. If the density difference is high, then the viscous forces are not playing any significant role and even the mobility ratio 100 behaves similar to that of mobility ratio 1. However if the density deference is less then few signs of channelling are witnessed. It is therefore concluded that increasing mobility in a low density difference case has negative effect while increasing mobility in a high density difference case has little or no effect with changing angular tilt.

Referring to the Figure 10 again for the cos (θ) values between 0 and -1 explains the same situation that changing angle producing little or no effect on a case if the density difference and mobility ratio is fixed. A respective line was therefore becomes approximately flat regardless of the change of angular tilt.

When the density difference is high, the mobility effect becomes suppressed and all the lines fall approximately on top of each other. However if the density difference is low then mobility ratio could be a sensitive parameter. Angular tilt in this case is not showing any sensitivity.

It is to be noted that throughout this sensitivity study, the definition of breakthrough concentration i.e. 0.2 mol/m^3 is used which might be too low especially for the cases when a light fluid is injected against the gravity. In these cases, buoyancy forces are more prominent and the light injected fluid can form channels through the porous model. As a result small concentration of the injected fluid can be sensed at the outlet boundary too early which results in constant breakthrough saturations at various angles between 120^o and 180^o.

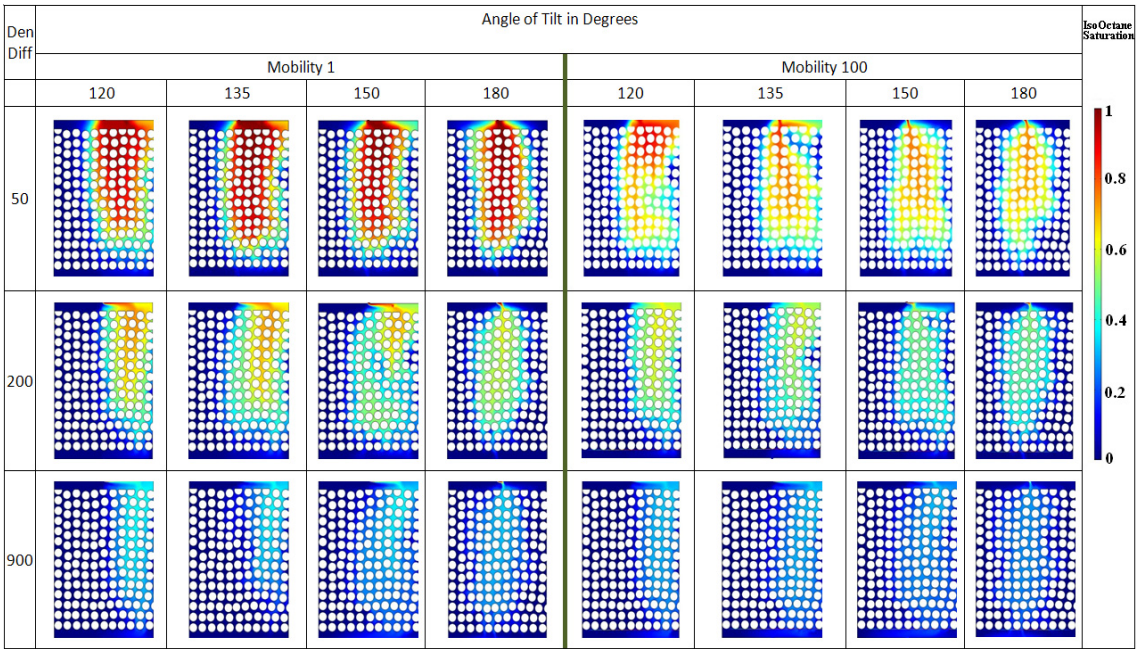

Figure 11. Comparison of different cases of region 2 with mobility ratio 1 and 100

5.2. Sensitivity Based on Domain Velocity

A sensitivity analysis was performed in order to evaluate the effect of the domain velocity on gravity dominated miscible displacement. A smaller velocity of 3.71x10^{-5} m/s was selected which represents a domain velocity of 0.4 ft/day by using equation 10. Since both velocities represent reservoir scale quantities, a significant change was not expected. The aim of investigating the effect of domain velocity is to evaluate whether or not velocity assists in gravity dominated miscible displacement process. A comparison has been made between the density differences starting from 50 kg/m^3 to 900 kg/m^3, mobility ratios ranging from 1 to 100, and for nine angles of tilt with respect to the vertical plane, which ranged from 0° to 180°. Figure 12 shows the plot of breakthrough saturation (Sb) versus cos (θ) for second velocity, where θ is the angle of tilt in degrees with respect to the vertical plane. Comparing Figure 10 and 12 showed that the reduction in the domain velocity ultimately reduces the inertial effects which decreases the value of breakthrough saturation compared with the case of higher velocity.

Further sensitivity will be made by increasing the velocity in the convection dominated regions to determine the role of convection on fluid displacement under gravity domination. In addition, sensitivity studies will be conducted based on the different grains arrangement.

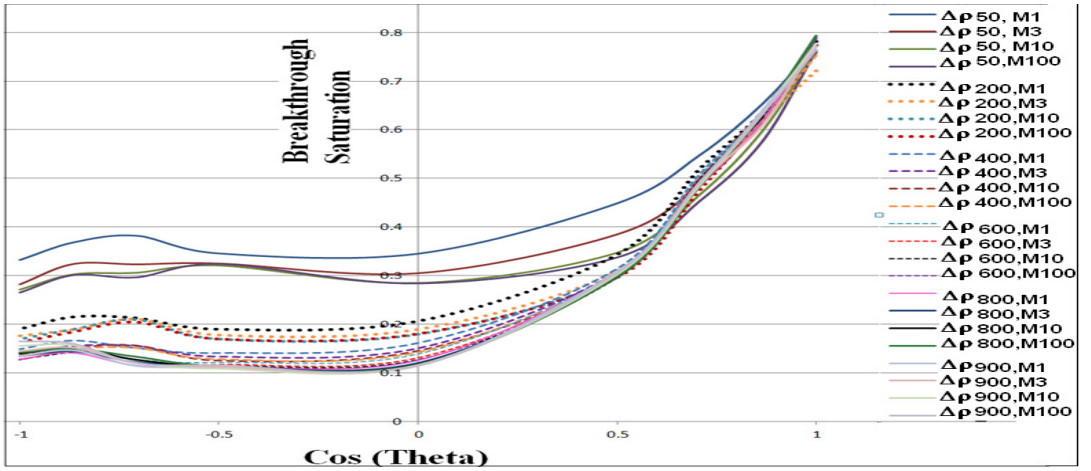

Figure 12. Breakthrough saturation Vs cos (θ) for range of mobility ratios and density differences using domain velocity of 0.4ft/day

6. Conclusion

- Pore scale study was conducted using same pattern on which experimental study was initially performed. This reduces the risk of uncertainty of using estimated pore geometry.
- Navier Stokes, Continuity Equation and Convection Diffusion were used in simulation study instead of pipe flow equations.
- In order to validate the simulation model Experimental results were matched based on the concentration in the porous domain.
- Detailed pore scale sensitivity study was conducted at various angular tilt, density differences, mobility ratios and domain velocities.
- Pore scale study suggests that when gravity is acting in favor of the displacement i.e. $0 \geq \theta \geq 90$, angular tilt is the most important parameter. Increasing θ significantly reduces the process efficiency. Mobility ratio could also be important factor if the density difference between injected and inplace fluid is small. However when gravity is acting against the displacing front, $90 > \theta \geq 180$, buoyancy forces are dominating and the increase in angular tilt does not produces significant effect on the process efficiency. Mobility ratio could be a sensitive parameter if the density difference is low. Furthermore inertial effects could be helpful for better sweep if the velocity remains in the dispersion domain.

7. Acknowledgement

Authors would like to acknowledge Mr Fahad Saleem Butt, Ms Fathima Mohamed Ali Sahib and Ms Lauren Brown who were attached with the project as Honours students. Authors also like to acknowledge Dr Themis Carageorgos for her assistance during the laboratory experiments.

8. References

1. Kurowski, P., C. Misbah, and S. Tchourkine, *Gravitational Instability of a Fictitious Front During Mixing of Miscible Fluids.* Europhys. Letters, 1995. **29** (4): p. 309
2. Tiffin, D.L. and V.J. KremesecJr., *Mechanistic Study of Gravity-Assisted CO_2 Flooding.* SPE Reservoir Engineering, 1988. **3** (2): p. 524-532.
3. Dumore, J.M., *Stability Considerations in Downward Miscible Displacements.* SPE Journal, 1964. **4**(4): p. 356 - 362.
4. Jadhawar, P.S. and H.K. Sarma, *Improved Production Strategy for Enhancing the Immiscible and Miscible CO_2-Assisted Gravity Drainage Oil Recovery*, in *International Oil and Gas Conference and Exhibition in China*. 2010: Beijing, China.
5. Kasiri, N. and A. Bashiri, *Gas-Assisted Gravity Drainage (GAGD) Process for Improved Oil Recovery*, in *International Petroleum Technology Conference*. 2009: Doha, Qatar.
6. Moore, J.S., *Design, Installation, and Early Operation of the Timbalier Bay S-2B(RA)SU Gravity-Stable, Miscible CO_2-Injection Project.* SPE Production Engineering, 1986. **1**(5): p. 369-378.
7. Palmer, F.S., A.J. Nute, and R.L. Peterson, *Implementation of a Gravity-Stable Miscible CO_2 Flood in the 8000 Foot Sand, Bay St. Elaine Field.* SPE Journal of Petroleum Technology, 1984. **36**(01): p. 101-110.
8. Bangia, V.K., F.F. Yau, and G.R. Hendricks, *Reservoir Performance of a Gravity-Stable, Vertical CO_2 Miscible Flood: Wolfcamp Reef Reservoir, Wellman Unit.* SPE Reservoir Engineering, 1993. **8**(4): p. 261-269.
9. Johnston, J.R., *Weeks Island Gravity Stable CO_2 Pilot*, in *SPE Enhanced Oil Recovery Symposium*. 1988: Tulsa, Oklahoma.
10. Hill, S., *Channeling in Packed Columns.* Chemical Engineering Science, 1952. **1**(6): p. 247-253.
11. Blackwell, R.J., J.R. Rayne, and W.M. Terry, *Factors Influencing the Efficiency of Miscible Displacement.* Petroleum Transactions, AIME, , 1959. **217**: p. 1-8
12. Gardner, G.H.F., J. Downie, and H.A. Kendall, *Gravity Segregation of Miscible Fluids in Linear Models.* SPE Journal, 1962. **2**(2): p. 95 - 104.
13. Slobod, R.L., *The Effects of Gravity Segregation in Laboratory Studies of Miscible Displacement in Vertical Unconsolidated Porous Media.* SPE Journal, 1964. **4**(1): p. 1-8.
14. Guo, T. and G.H. Neale, *Effects of Buoyancy Forces on Miscible Liquid-Liquid Displacement Processes in a Porous Medium.* Powder Technology, 1996. **86**(3): p. 265-273.
15. Page, C.A., H.J. Brooks, and G.H. Neale, *Visualization of the Effects of Buoyancy on Liquid-Liquid Displacements in Vertically Aligned Porous Medium Cells.* Experiments in Fluids, 1993. **14**(6): p. 472-474.
16. Mahmoud, T. and D.N. Rao, *Mechanisms and Performance Demonstration of the Gas-Assisted Gravity-Drainage Process using Visual Models* in *SPE Annual Technical Conference and Exhibition 2007, California, U.S.A.* 2007.
17. Jiao, C. and T. Maxworthy, *An Experimental Study of Miscible Displacement with Gravity-Override and Viscosity-Contrast in a Hele Shaw cell.* Experiments in Fluids, 2008. **44**(5): p. 781-794.
18. Mohiuddin, Z. and M. Haghighi, *Visualization of CO_2 Displacement Process under Gravity Domination*, in *SPE Enhanced Oil Recovery Conference, Kuala Lumpur, Malaysia*. 2011.
19. Mohiuddin, Z., et al., *Pore Scale Visualization and Simulation of Miscible Displacement Process under Gravity Domination*, in *International Petroleum Technology Conference*. 2012: Bangkok, Thailand.
20. Fatt, I., *The Network Model of Porous Media.* Petroleum Transactions, AIME, 1956. **207** p. 144-181

21. Rose, W., *Studies of Waterflood Performance III - Use of Network Models* Circular 237, Division of Illinois State Geological Survey, Urbana 1957.

22. Simon, R. and F.J. Kelsey, *The Use of Capillary Tube Networks in Reservoir Performance Studies: 1. Equal-Viscosity Miscible Displacements.* SPE Journal, 1971. **11**(2): p. 99-112.

23. Mollaei, A., M. Haghighi, and B.B. Maini, *Experimental Investigation and Network Modeling Simulation of Free Fall Gravity Drainage in Single-Matrix and Fractured-Blocks Models*, in *Abu Dhabi International Petroleum Exhibition and Conference*. 2006: Abu Dhabi, UAE.

24. Stevenson, K., et al., *2-D Network Model Simulations of Miscible Two-Phase Flow Displacements in Porous Media: Effects of Heterogeneity and Viscosity*. Physica A: Statistical Mechanics and its Applications, 2006. **367**: p. 7-24.

25. Blunt, M.J., *Flow in Porous Media -- Pore-Network Models and Multiphase Flow.* Current Opinion in Colloid and Interface Science, 2001. **6**(3): p. 197-207.

26. Xu, J.Q., *Modeling Unsteady-State Gravity-Driven Flow in Porous Media.* Journal of Petroleum Science and Engineering, 2008. **62**(3-4): p. 80-86.

27. Lenormand, R., E. Touboul, and C. Zarcone, *Numerical Models and Experiments on Immiscible Displacements in Porous Media.* Journal of Fluid Mechanics, 1988. **189**: p. 165-187.

28. Xu, B., et al., *Use of Pore-Network Models to Simulate Laboratory Corefloods in a Heterogeneous Carbonate Sample.* SPE Journal, 1999. **4**(3): p. 178-186.

29. Stevenson, K., *MSc Thesis :Miscible Network Model 2-D Simulations of Two-Phase Flow Displacements in Porous Media with Gravitational and Distributional Effects*, in *Department of Statistics*. 2004, West Virginia University.

30. Fayers, F.J., R.I. Hawes, and J.D. Mathews, *Some Aspects of the Potential Application of Surfactants or CO_2 as EOR Processes in North Sea Reservoirs.* SPE Journal of Petroleum Technology, 1981. **33**(9): p. 617-1627.

31. Stalkup, F.I.J., *Miscibile Displacement -SPE Monograph volume 8*. 1983.